Ferric Iron Content of Mineral Inclusions in Diamonds from São Luiz: A View into the Lower Mantle

Catherine McCammon*, Mark Hutchison, Jeff Harris

Mössbauer spectroscopy on inclusions in diamonds from São Luiz, Brazil, show that (Mg,Fe)O inclusions contain little Fe^{3+} ($Fe^{3+}/\Sigma Fe \leq 7\%$), whereas inclusions with pyroxene composition (believed to have been originally in the perovskite structure) and tetragonal almandine-pyrope phase (TAPP) inclusions contain high relative amounts of Fe^{3+} ($Fe^{3+}/\Sigma Fe = 20$ to 75%). These observations are consistent with high-pressure experiments on synthetic samples and support the idea that the inclusions originated in the lower mantle. Fe-Mg partitioning data for co-existing $(Mg,Fe,Al)(Si,Al)O_3$ – (Mg,Fe)O pairs also indicate that the phases were in equilibrium at the time of diamond formation in the lower mantle.

Samples from the Earth's mantle provide important geochemical data for assessing the nature of the Earth's interior. Properties such as oxygen fugacity can be constrained by observations on natural samples; therefore, we know more about the composition of the upper mantle than the lower mantle, where we have been restricted until recently to inferences from experiments and theory. The discovery of $(Mg,Fe,Al)(Si,Al)O_3$, (Mg,Fe)O, $CaSiO_3$, and tetragonal almandine-pyrope phase (TAPP) inclusions in diamonds from São Luiz River, Brazil (*1*–*3*), provides an opportunity to investigate directly the oxidation state of minerals believed to have originated in the lower mantle. These phases form a stable assemblage only at pressures and temperatures equivalent to those in the lower mantle; at lower pressure they would combine to form phases with olivine, garnet, or pyroxene stoichiometry (*4*). Diamond tends to preserve the chemistry of mineral phases at the conditions of diamond formation, and examination of fracture systems around inclusions, determination of internal pressures within the inclusions, and stable isotope studies indicate that the São Luiz diamonds have likely preserved their chemical state during exhumation and have not been contaminated during transport (*5*). The $(Mg,Fe,Al)(Si,Al)O_3$ inclusions are believed to have existed as a perovskite phase in the lower mantle, whereas TAPP is believed to be primary (*3*). Here, we use a technique in which Mössbauer spectroscopy is performed on microscopic absorbers (*6*) to study the oxidation state ($Fe^{3+}/\Sigma Fe$) of these inclusions. Although the extent to which the São Luiz inclusions represent the bulk lower mantle is not yet clear, they represent an opportunity to study samples that have equilibrated in a natural multiphase system at pressures and temperatures believed to be within the lower mantle. Results can be used to assess the oxygen fugacity in the region of diamond formation.

Inclusions greater than 60 μm in diameter were extracted by crushing from diamonds that showed no visible fractures between the inclusion and the diamond surface. The inclusions were mounted in epoxy and polished for electron microprobe analysis (*7*) (Table 1). In one diamond (BZ251), a surface was polished to expose the inclusions. The samples could be used for Mössbauer analysis with no further modification (*8*).

Mössbauer spectra of the (Mg,Fe)O inclusions are similar to spectra of synthetic samples (*9*) and consist of a broad quadrupole doublet with a shoulder at low velocity corresponding to Fe^{3+} absorption (*10*). The relative amount of Fe^{3+} in all (Mg,Fe)O inclusions is uniformly low, with the exception of sample BZ66, which shows a slightly higher value (Table 1). This could be related to the higher Na concentration, where the charge deficit from substitution of a small amount of Na^+ is compensated by Fe^{3+}.

The small amounts of Fe^{3+} in the (Mg,Fe)O inclusions are consistent with results from high-pressure experiments on (Mg,Fe)O that demonstrate that the solubility of Fe^{3+} is dramatically reduced at high pressure, likely as a result of a phase transition in the system Fe_3O_4-$MgFe_2O_4$ (*11*). Stabilization of Fe^{3+} in the dense $(Mg,Fe)Fe_2O_4$ phase means that (Mg,Fe)O should contain only a small amount of Fe^{3+} at pressure and temperature conditions of the lower mantle, regardless of the oxygen fugacity.

In contrast, the $(Mg,Fe,Al)(Si,Al)O_3$ and TAPP inclusions contain extremely high relative amounts of Fe^{3+} (Table 1). Mössbauer spectra from the $(Mg,Fe,Al)(Si,Al)O_3$ and TAPP inclusions are similar; both were fitted to an Fe^{2+} doublet with large quadrupole splitting and an Fe^{3+} doublet with small quadrupole splitting. The high-velocity component of the Fe^{3+} doublet is well resolved, allowing an unambiguous determination of the Fe^{3+} content.

The hyperfine parameters from spectra of the $(Mg,Fe,Al)(Si,Al)O_3$ inclusions (Table 2) are similar to those of Al silicate glasses (*12*), but quite different from those

Table 1. Chemical composition (in weight percent) of São Luiz inclusions examined using Mössbauer spectroscopy.

Sample	(Mg,Fe)O					$(Mg,Fe,Al)(Si,Al)O_3$		TAPP	
	BZ66	BZ67	BZ73	BZ238B	BZ251A	BZ210B	BZ251B	BZ238A	BZ243A
SiO_2	0.01	0.00	0.02	0.07	0.04	51.41	57.04	41.41	42.24
TiO_2	0.01	0.01	0.02	0.04	0.01	0.02	0.15	0.03	0.04
Al_2O_3	0.13	0.06	0.04	0.12	0.04	10.04	1.33	23.33	24.17
Cr_2O_3	1.06	0.03	0.38	0.66	0.34	1.19	0.40	2.99	2.41
FeO	68.41	58.61	42.49	25.58	23.52	1.28	3.04	1.29	1.76
Fe_2O_3*	5.72	1.33	0.96	0.88	0.00	4.28	0.84	4.10	3.81
MnO	0.80	0.28	0.10	0.36	0.22	0.93	0.14	0.92	0.90
NiO	0.10	0.28	0.40	1.40	1.25	0.02	0.00	0.01	0.02
MgO	23.13	39.75	56.37	71.31	74.77	30.21	36.25	24.95	24.36
CaO	0.01	0.00	0.00	0.00	0.02	0.65	0.06	0.13	0.11
Na_2O	1.05	0.11	0.06	0.12	0.18	1.05	0.03	0.16	0.09
K_2O	0.00	0.00	0.00	0.00	0.01	0.26	0.02	0.02	0.00
Total	100.44	100.46	100.82	100.55	100.38	101.35	99.30	99.34	99.92
Approx. diam. (μm)	100	150	300	150	100	60	100	60	60
Fe/(Mg+Fe)	64.1	45.8	30.1	17.2	15.0	8.7	5.6	10.1	10.7
$Fe^{3+}/\Sigma Fe$ (%)	7(2)	2(2)	2(1)	3(3)	0(2)	75(3)	20(6)	74(8)	66(8)

*Corrected value based on Mössbauer spectroscopy results.

C. McCammon, Bayerisches Geoinstitut, Universität Bayreuth, D-95440 Bayreuth, Germany.
M. Hutchison, Department of Geology and Geophysics, University of Edinburgh, West Mains Road, Edinburgh EH9 3JW, UK.
J. Harris, Department of Geology and Applied Geology, University of Glasgow, Glasgow G12 8QQ, UK.
*To whom correspondence should be addressed.

of crystalline orthopyroxene (*13*). The inclusions were observed to be isotropic under a polarizing microscope, consistent with an amorphous structure. These results are consistent with an origin of these phases as lower mantle perovskite, which is known from experimental studies to transform readily to glass, particularly for iron-containing compositions (*14*). The Fe^{2+} hyperfine parameters of the TAPP inclusions are consistent with octahedral coordination, and would suggest that most of the Fe^{2+} is in either the M1 or M3 sites in the TAPP structure, or both. The smaller size of the M2 site would likely result in a smaller center shift than the one observed; therefore, significant occupation of the M2 site by Fe^{2+} is less likely. The Fe^{3+} hyperfine parameters suggest that Fe^{3+} occupies either a tetrahedral site or a distorted octahedral site (*15*). Because less than half the available Fe^{3+} would be required to fill the Si tetrahedral sites in TAPP for full occupancy (*3*), the latter possibility seems more likely. The site assignments from the Mössbauer hyperfine parameters are consistent with those proposed by Harris *et al.* (*3*) from single crystal refinements of TAPP.

The large amounts of Fe^{3+} in the silicate phases are consistent with recent results demonstrating that Al^{3+} stabilizes Fe^{3+} in the perovskite structure (*16*). A likely mechanism is through the substitution $Mg^{2+} + Si^{4+} \rightarrow Al^{3+} + Fe^{3+}$ which maintains electrostatic charge balance in the crystal structure (Fig. 1). The structure of TAPP is more complex than that of perovskite but has the same possibility for charge compensation.

Results from Mössbauer spectroscopy provide additional evidence that the inclusions from the São Luiz suite originated in the lower mantle. The low Fe^{3+} content of the (Mg,Fe)O inclusions can only be reconciled with the high Fe^{3+} content of the silicate inclusions if the inclusions formed at conditions of the lower mantle. If the (Mg,Fe)O inclusions formed at low pressure, phase relations in the FeO-MgO-Fe_2O_3 system imply that the oxygen fugacity would have to be near Fe equilibrium to obtain such low Fe^{3+} concentrations (*17*). Such low oxygen fugacities would produce low $Fe^{3+}/\Sigma Fe$ values in the silicate phases, however. It is only under lower mantle conditions that Fe^{3+} is stabilized in the perovskite phase to produce the observed $Fe^{3+}/\Sigma Fe$ values in the silicate inclusions from São Luiz. One other possibility to explain the high values of $Fe^{3+}/\Sigma Fe$ in the $(Mg,Fe,Al)(Si,Al)O_3$ phase would be oxidation of Fe^{2+} in the amorphous phase on decompression as observed in silicate melts (*18*), but this would appear unlikely based on the TAPP results and the observed effect of Al on Fe^{3+} content and Fe/Mg partitioning as expected for the perovskite phase.

Fe/Mg partitioning data are consistent with formation of the São Luiz inclusions at lower mantle pressures and temperatures. High-pressure experiments on the assemblage (Mg,Fe)O–$(Mg,Fe,Al)(Si,Al)O_3$ perovskite show that preferential partitioning of Fe into (Mg,Fe)O is dramatically reduced in the presence of Al (*19*). A number of (Mg,Fe)O–$(Mg,Fe,Al)(Si,Al)O_3$ pairs coexist in the same diamond in the São Luiz suite. Fe-Mg partition coefficients calculated from electron microprobe analyses (Fig. 2) decrease with increasing Al content, consistent with the expected effect of oxidizing Fe^{2+} to Fe^{3+} (the electron microprobe analyzes only total iron; hence the partition coefficient appears to decrease). The results are also consistent both with recent high-pressure experiments on samples with pyrolite composition (*20*) and the only $(Mg,Fe,Al)(Si,Al)O_3$–(Mg,Fe)O inclusion pair reported to occur outside the São Luiz suite (*21*). A modest extrapolation of the inclusion data to zero Al content gives a partition coefficient near 3, which is consistent with experiments in Al-free systems (*22*).

High-pressure experiments have shown that values of $Fe^{3+}/\Sigma Fe$ are high in $(Mg,Fe,Al)(Si,Al)O_3$ perovskite regardless of whether synthesis occurred under oxidizing or reducing conditions (*16, 23*), although the latter case requires charge compensation such as through the disproportionation reaction $Fe^{2+} \rightarrow Fe^{3+} + Fe^0$ or the production of significant lattice defects. High-pressure experiments on (Mg,Fe)O indicate that $Fe^{3+}/\Sigma Fe$ remains relatively low regardless of oxygen fugacity, because Fe^{3+} is believed to be stabilized in a high-pressure form of the $(Mg,Fe)Fe_2O_4$ spinel phase, which exsolves from (Mg,Fe)O. This would imply that (Mg,Fe)O equilibrated at higher oxygen fugacities should have a greater abundance of exsolved $(Mg,Fe)Fe_2O_4$. The oxygen fugacity conditions existing at the time of diamond formation in the lower mantle can therefore be assessed from the microstructures of (Mg,Fe)O and $(Mg,Fe,Al)(Si,Al)O_3$ inclusions. Although definitive conclusions must await detailed analysis, results suggesting the presence of $(Mg,Fe)Fe_2O_4$ in (Mg,Fe)O inclusions (*24*) and the lack of metallic Fe or significant oxygen defects in $(Mg,Fe,Al)(Si,Al)O_3$ inclusions suggest that the inclusions formed under conditions of oxygen fugacity are significantly higher than Fe equilibrium.

Table 2. Hyperfine parameters from Mössbauer spectra of São Luiz silicate inclusions. The numbers in parentheses refer to the standard deviation of the last digit.

Sample	Center shift* (mm/s)	Quadrupole splitting (mm/s)	Line width (mm/s)
Fe^{2+}			
210B	1.20(2)	2.30(4)	0.35†
251B	1.16(5)	2.23(9)	0.36(5)
238A	1.03(19)	2.39(39)	0.35†
243A	1.10(3)	2.04(6)	0.35†
Fe^{3+}			
210B	0.13(1)	0.56(2)	0.33(2)
251B	0.20(11)	0.30(22)	0.26(14)
238A	0.15(8)	0.57(15)	0.38(5)
243A	0.17(2)	0.69(3)	0.39(5)

*Relative to Fe metal. †Line width fixed during fitting.

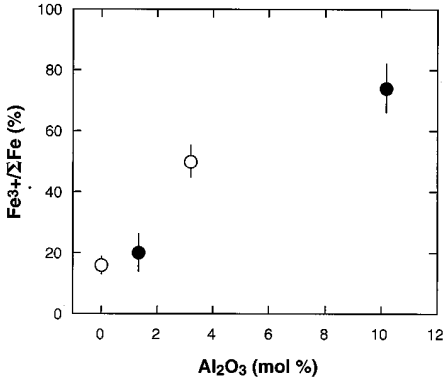

Fig. 1. Variation of $Fe^{3+}/\Sigma Fe$ with Al content of $(Mg,Fe)SiO_3$ perovskite. Open circles are from previously reported multianvil experiments (*16*) and solid circles are from São Luiz diamond inclusions (present work). Iron compositions [expressed as Fe/(Fe+Mg)] of the $(Mg,Fe,Al)(Si,Al)O_3$ and perovskite phases range between 5 and 9%.

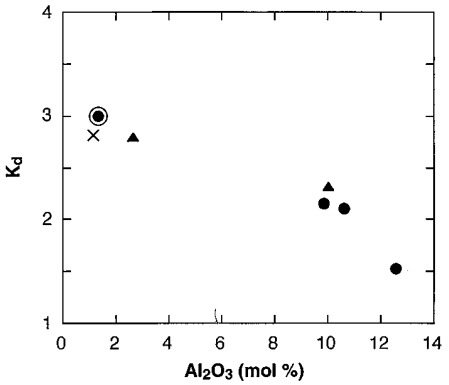

Fig. 2. Variation of Fe-Mg partition coefficient between $(Mg,Fe,Al)(Si,Al)O_3$ and (Mg,Fe)O inclusions [$K_d = (X^{mw}_{Fe}/X^{mw}_{Mg})/(X^{Pv}_{Fe}/X^{Pv}_{Mg})$] with Al content. Solid circles are from São Luiz electron microprobe data from (*24*), where the outlined circle indicates the pair examined by Mössbauer spectroscopy in the present study (BZ251). Solid triangles are from São Luiz electron microprobe data of (*2*). The cross refers to the only known $(Mg,Fe,Al)(Si,Al)O_3$–(Mg,Fe)O inclusion pair not from São Luiz (*21*).

REFERENCES AND NOTES

1. M. C. Wilding, B. Harte, J. W. Harris, *Proc. 5th Int. Kimberlite Conf.* (1991), p. 456.
2. B. Harte and J. W. Harris, *Mineral. Mag.* **58A**, 384 (1994).
3. J. W. Harris, M. T. Hutchison, M. Hursthouse, M. Light, B. Harte, *Nature* **387**, 486 (1997).
4. E. Ito, E. Takahashi, Y. Matsui, *Earth Planet. Sci. Lett*. **67**, 238 (1984).
5. M. T. Hutchison, B. Harte, J. W. Harris, I. Fitzsimons, *6th Int. Kimberlite Conf.* (abstr.) (1995), p. 242.
6. To obtain adequate count rates, the conventional Mössbauer source (typical specific activity 100 mCi/cm^2) is replaced by a point source (specific activity $>$ 2000 mCi/cm^2). The gamma rays are collimated to the selected sample diameter using a Pb shield, and the source-sample distance is reduced to $<$5 mm. The latter results in a solid angle similar to conventional experiments, and hence a similar count rate. Because the signal quality depends on absorber density (measured in milligrams of Fe per square centimeter) and not the total amount of iron in the sample, the reduction in sample size has no effect on the effective thickness of the absorber. When electronic absorption due to heavier elements is low and the point source is relatively new ($<$1 year old), high-quality Mössbauer spectra (comparable to conventional measurements) can be recorded on samples with diameters as small as 100 μm. For further information see C. A. McCammon, V. Chaskar, and G. G. Richards [*Meas. Sci. Technol*. **2**, 657 (1991)] and C. A. McCammon [*Hyper. Int.* **92**, 1235 (1994)].
7. Compositions were determined using a Cameca Camebax electron microprobe at the University of Edinburgh, Department of Geology and Geophysics, operating at 20 kV with a beam current of 20 nA.
8. The epoxy disks were mounted with cellophane tape behind a 200- to 500-μm-diameter hole drilled in 25-μm- thick Ta foil. The foil acts as a collimator, absorbing more than 99% of the 14.4-keV gamma rays. Absorber densities based on the thickness of the samples and chemical compositions were $>$ 10 mg of Fe per square centimeter for the (Mg,Fe)O inclusions, and approximately 1 mg of Fe per square centimeter for the (Mg,Fe,Al)(Si,Al)O_3 and TAPP inclusions. Mössbauer spectra were collected for times ranging from 1 day for the (Mg,Fe)O inclusions to more than 20 days for the silicate inclusions. Mössbauer spectra were recorded at room temperature in transmission mode on a constant acceleration Mössbauer spectrometer with a nominal 20 mCi of ^{57}Co high specific activity source (2 Ci/cm^2) in a 12-μm Rh matrix. The velocity scale was calibrated relative to 25-μm α-Fe foil using the positions certified for National Bureau of Standards standard reference material no. 1541; line widths of 0.42 mm/s for the outer lines of α-Fe were obtained at room temperature. The spectra were fitted to Lorentzian and Voigt line shapes using the commercially available fitting program NORMOS written by R.A. Brand (distributed by Wissenschaftliche Elektronik GmbH, Germany).
9. V. V. Kurash *et al*., *Inorg. Mater.* **8**, 1395 (1972).
10. We fitted Mössbauer spectra of (Mg,Fe)O to two Fe^{2+} doublets and one Fe^{3+} singlet, all with Voigt line shape. The area of Fe^{3+} absorption is constrained by the asymmetry of the main doublet, and is therefore relatively independant of the fitting model.
11. C. A. McCammon, J. W. Harris, B. Harte, M. T. Hutchison, in *Plume 2*, D. L. Anderson, S. R. Hart, A. W. Hofmann, Eds. [*Terra Nostra* **3**, 91 (1995)].
12. F. Seifert, B. O. Mysen, D. Virgo, E.-R. Neumann, *Annu. Rep. Carneg. Inst. Wash. Geophys. Lab*. **81**, 355 (1982).
13. H. Annersten, M. Olesch, F. A. Seifert, *Lithos* **11**, 301 (1978).
14. Y. B. Wang, F. Guyot, R. C. Liebermann, *J. Geophys. Res.* **97**, 12, 327 (1992).
15. C. A. McCammon, *Phase Trans.* **58**, 1 (1996); G. M. Bancroft, A. G. Maddock, R. G. Burns, *Geochim. Cosmochim. Acta* **31**, 2219 (1967).
16. C. A. McCammon, *Nature* **387**, 694 (1997).
17. D. H. Speidel, *J. Am. Ceram. Soc.* **50**, 243 (1967).
18. M. Brearly, *J. Geophys. Res.* **B10**, 15703 (1990).
19. B. J. Wood and D. C. Rubie, *Science* **273**, 1522 (1996).
20. T. Irifune and M. Isshiki, paper presented at the International Conference on High-Pressure Science and Technology (AIRAPT-16 and HPCJ-38), Kyoto, Japan (1997), p. 169.
21. R. O. Moore, M. L. Otter, R. S. Rickard, J. W. Harris, J. J. Gurney, *Geol. Soc. Aust. Abstr.* **16**, 409 (1986).
22. F. Guyot, M. Madon, J. Peyronneau, J. P. Poirier, *Earth Planet. Sci. Lett.* **90**, 52 (1988); Y. Fei, H. K. Mao, B. O. Mysen, *J. Geophys. Res*. **96**, 2157 (1991); S. E. Kesson and J. D. Fitz Gerald, *Earth Planet. Sci. Lett.* **111**, 229 (1991).
23. S. Lauterbach, C. A. McCammon, F. Seifert, paper presented at the 75th annual meeting of the German Mineralogical Society, Cologne, Germany, 15 to 19 September 1997.
24. M. Hutchinson, in preparation.

25. The mineral inclusions were supplied by B. Harte, and the electron microprobe analyses for samples BZ66, BZ67, BZ73, and BZ210B were performed by M. Wilding and B. Harte. The manuscript was improved through discussions with B. Harte and S. Kesson.

3 July 1997; accepted 18 August 1997

Triton's Distorted Atmosphere

J. L. Elliot,* J. A. Stansberry, C. B. Olkin, M. A. Agner, M. E. Davies

A stellar-occultation light curve for Triton shows asymmetry that can be understood if Triton's middle atmosphere is distorted from spherical symmetry. Although a globally oblate model can explain the data, the inferred atmospheric flattening is so large that it could be caused only by an unrealistic internal mass distribution or highly supersonic zonal winds. Cyclostrophic winds confined to a jet near Triton's northern or southern limbs (or both) could also be responsible for the details of the light curve, but such winds are required to be slightly supersonic. Hazes and clouds in the atmosphere are unlikely to have caused the asymmetry in the light curve.

Data from the Voyager 2 encounter with Triton in August 1989 (*1*) showed that Triton's atmosphere is dynamic on short time scales. Dark plumes rose from the surface to an altitude of 8 km and were observed to drift downwind for more than 100 km (*2*). Wind streaks on the surface in the southern hemisphere indicated a northeasterly flow near the ground with wind speeds of 5 to 15 m s^{-1} (*3*). Discrete clouds were seen up to 8 km above the surface, and haze was detected up to altitudes of 20 to 30 km (*4*). Because Triton's predominantly N_2 atmosphere is in vapor-pressure equilibrium with the surface ice (the heat of vaporization and condensation equalize the surface temperature on Triton), seasonal changes in insolation can produce changes in surface pressure of several orders of magnitude (*5*). The thermal structure of Triton's middle atmosphere is probably controlled by a steady-state balance of heat input from the sun and magnetospheric electrons, radiative processes involving CH_4 and CO, and thermal conduction to the surface (*6*). On the basis of the plumes, the lower 8 km of the atmosphere has been modeled as a troposphere (*7*).

To test atmospheric models based on Voyager data and to measure the predicted changes in surface pressure with time, we began monitoring Triton's atmosphere with a series of Earth-based stellar occultation observations in 1993. The results of these observations (*8*) are not consistent with the temperature and pressure predicted by models (*6*) at an altitude of 90 km. For the 14 August 1995 occultation discussed here, the Infrared Telescope Facility (IRTF) was situated close enough to the center of Triton's occultation shadow to record the partial focusing of starlight by Triton's atmosphere—a phenomenon known as the "central flash" (*9*). The central-flash ray-paths probe several scale heights deeper into the atmosphere than the main immersion and emersion light curves of the occultation. They also sample large portions of the planetary limb, making the central flash a tool that has been used to investigate the properties of winds and extinction (particulate and molecular) in the atmospheres of Mars, Saturn, Titan, and Neptune (*10*, *11*).

The visible wavelength occultation data (Fig. 1) exhibit two asymmetries in the light

J. L. Elliot, Department of Earth, Atmospheric, and Planetary Sciences and Department of Physics, Building 54-422, Massachusetts Institute of Technology, 77 Massachusetts Avenue, Cambridge, MA 02139–4307, USA; and Lowell Observatory, 1400 West Mars Hill Road, Flagstaff, AZ 86001–4499, USA.
J. A. Stansberry and C. B. Olkin, Lowell Observatory, 1400 West Mars Hill Road, Flagstaff, AZ 86001–4499, USA.
M. A. Agner, Department of Earth, Atmospheric, and Planetary Sciences, Building 54-314, Massachusetts Institute of Technology, 77 Massachusetts Avenue, Cambridge, MA 02139–4307, USA.
M. E. Davies, RAND Corporation, 1700 Main Street, Santa Monica, CA 90407–3297, USA.

*To whom correspondence should be addressed at the Department of Earth, Atmospheric, and Planetary Sciences, Building 54-422, Massachusetts Institute of Technology, 77 Massachusetts Avenue, Cambridge, MA 02139–4307, USA. E-mail: jle@mit.edu